Progress towards Understanding the Charge Transport Hopping Mechanism in Molecularly Doped Polymers

L.B Schein, Independent Consultant, San Jose, CA (USA); Andrey Tyutnev, Moscow State Institute of Electronics and Mathematics, Trekhsvyatitel'skii per. 3/12, Moscow (Russia); D. S. Weiss, Department of Chemical Engineering, University of Rochester, Rochester, New York (USA)

Abstract

Recent progress towards understanding the charge transport mechanism in molecularly doped polymers MDP is reviewed. It has already been shown that the mobility is not understandable in terms of the Gaussian Disorder Model (GDM) or any other available model. In this paper, it is shown that characteristic features of the current-time transient are also not understandable in terms of available models. In addition, a method has been used to convert disorder energies obtained from GDM into Arrhenius activation energies. Using this methodology a list has been compiled of the activation energies of all molecularly doped polymers which have been characterized as a function of dopant concentration. This list demonstrates that disorder and polaron binding energies are small compared to observed activation energies, suggesting that some higher energy process determines the charge transport mechanism in MDP. The experimental observations of activation energies that depend on ρ, the distance between hoping sites, and pre-factors independent of ρ are attributed to either interactions among the dopant molecules or the failure of the lattice gas model to properly calculate ρ at high dopant concentrations.

Introduction

The organic photoreceptor OPC used in virtually all electrophotographic engines is made up of a thin charge generation layer and a thick charge transport layer made from a molecularly doped polymer MDP. The mechanism of charge transport in the MDP has been under discussion for many years. Most papers have used the Gaussian Disorder Model GDM to explain experimental data. The GDM envisions the charge carriers hopping in a Gaussian distribution of states through the MDP aided by the imposed electric field. The width of the Gaussian distribution of states is directly determined by the disorder in the material.

Recent Progress

In the last two years a series of papers have compared the GDM and other transport theories to the whole body of experimental data, instead of focusing on one material at a time. When this was done, it was found that (1) the GDM does not adequately describe charge transport data in MDP because the disorder energy, which can be obtained from the temperature dependence of the mobility, does not change as predicted by the theory when the disorder is changed [1], (2) the shape of the transient current also is not understandable in terms of any known transport theory [2], and (3) the activation energy scale, which has been derived from the disorder energies, is approximately 0.3-0.8 eV, which is larger than predicted for the disorder or the polaron binding energies [3]. The experimental observations of activation energies that depend on ρ, the distance between hoping sites, and pre-factors independent of ρ are attributed to either interactions among the dopant molecules or the failure of the lattice gas model to properly calculate ρ at high dopant concentrations [3]. It appears that something critical is missing from our understanding of charge transport in MDP and perhaps in all organic materials.

GDM Does Not Adequately Describe Charge Transport Data

The primary argument that led to this conclusion is that the disorder energy, which can be obtained from the temperature dependence of the mobility, does not change as predicted by the theory when the disorder is changed. The detailed discussion was presented last year at NIP 24 [4] and in Ref. 1.

The Current Transient is Not Understandable in Terms of Current Theories

To illustrate the discussion in Ref. 2 concerning the current transients, consider the shape of the transient conductivity pulse in standard linear current-linear time axes (see Fig.1). The data were taken with an electron gun excitation of 7 KeV, which generated holes within the first 1 micron of the sample. The plot on linear-linear axes is familiar: an initial spike followed by a relatively flat current before the transit time; a mobility that follows the Poole-Frenkel law, being exponential in the square root of the electric field; and a current after the transit time that falls much more slowly than can be accounted for using Gaussian statistics. Other data from this sample are shown in Fig. 2-4; this sample has no prior history of e-beam excitation before this experiment and the data from this sample have been repeated many times on other samples. Data at the same electric field are plotted using log-log axes in Fig. 2. This figure reveals the behavior over long times and low currents. Before the transit time the decrease of the current can be characterized by two power laws, $t^{-0.3}$ which is the time t dependence of the spike, and approximately t^0, which is the time dependence of the plateau. The current only decreases by about a factor of 2 from 10^{-2} of the transit time to the transit time. After the transit time the current decreases algebraically as $t^{-2.2}$ to a current value of about 10^{-2} of the value at the transit time. The current shape is universal, which means it is independent of electric field. This is shown in Fig. 3 and 4. In Fig. 3 are shown w as a function of electric field. w is defined as $(\tau_{1/2}-\tau_0)/\tau_{1/2}$, where τ_0 is the transit time and $\tau_{1/2}$ is the time at which the current falls to half the value at the transit time. Note that w is independent of electric field, an indication of universality. Fig. 4 shows an overlay of three electric fields from 2.5 to 33 V/μm normalized to the

transit time on a log-log plot. It is an even stronger test of universality: the curves are independent of electric field from very short times, which includes the spike, to very long times (consistent with Fig. 3). We suggest calling this strong universality.

Available theoretical models are not consistent with these data.

The nearly constant current before the transit time suggests that the carriers are hopping with an approximately constant mobility by some intrinsic hopping mechanism or they are in dynamic equilibrium with an intrinsic shallow trap. A small decease in slope could indicate that a small amount of deep trapping exists with a very long release time (with respect to the transit time). This is consistent with the known temperature dependence of this current: it decreases more steeply as the temperature is lowered. But the origin of the initial spike and its time dependence, $t^{-0.3}$, are not understood.

The behavior after the transit time is puzzling. Attempts to explain this behavior with all known theories have failed to account for it. It is much wider than Gaussian transport would predict and it is not consistent with the width being determined by the generation region, Rudenko and Arkhipov's field diffusion model, Coulomb repulsion, or an intrinsic shallow-trap controlled mobility [2].

The data are inconsistent with the predictions of the GDM (putting aside the difficulties that the GDM has explaining the electric field dependence of the mobility and the experimental effects of changing disorder on the activation energy) because the slope of the current before the transit time is observed to be more shallow than predicted and because the field independence of slope is not predicted. Field independent slopes appear to be a general phenomenon of molecularly doped polymers (Fig. 3, 4, and Ref 2.)

The data are inconsistent with the Scher-Montrol theory that assumes waiting time distribution functions which are longer than the transit time and its predicted electric field dependence [2].

Energy Scales

The third paper [3] deals with the confusion caused by the disagreement on the role of disorder, which has led to disagreement on how to analyze the experimental mobility data. Plotting the mobility vs. T^{-1} or T^{-2} where T is temperature gives activation energies or disorder energies respectively, which cannot be compared. Methods of obtaining the activation energy from the disorder energy have been suggested and implemented [3]. The results are shown in Tables 1 and 2. The activation energies in bold are directly measured; those in normal print are calculated from the disorder energies. The results are that the activation energies are between 0.3-0.8 eV. These results provide new evidence that disorder is of secondary importance in charge transport phenomena in MDP. The estimated largest dipolar disorder energy, 0.14 eV for a material with the largest dipole moment, 5.78 D, at the highest concentration reported, 60% DNTA in PC, is small compared to observed activation energies. Disorder energies for all other materials (with lower dipole moment) and lower concentration should be smaller than this value. Calculated polaron binding energies are also small [5], 0.3 ± 0.1 eV compared to experimental observations (the polaron binding energy should be twice the observed activation energy or 0.6-1.6 eV), suggesting that polarons do not govern charge transport in molecularly doped polymers. The large values of the observed activation energies suggest that some higher energy process determines the charge transport mechanism in MDP.

Given the uniformity of behavior of the mobility in the MDP's of Table 1 and 2 with respect to electric field, temperature, current shape, and sample thickness, we do not find it reasonable that there are two types of mobility characteristics in MPD's which are represented by Table 1 and Table 2, those that have an activation energy that is independent of dopant concentration (Table 1) and those that have an activation energy that depends on dopant concentration (Table 2). It is argued [3] that the intrinsic mobilities in MDP's are activated, with an activation energy that is independent of dopant concentration, and have a pre-factor that is exponential in ρ, the calculated distance between hoping sites, as expected for a hoping theory. The experimental observations of other behaviors, activation energies that depend on ρ (see Table 2) and pre-factors independent of ρ (Ref. 1 and 3), are attributed to either interactions among the dopant molecules or the failure of the lattice gas model to properly calculate ρ at high dopant concentrations. Therefore only the high values of activation energies in Table 2 are used to determine the energy scale – the lower vales are determined by interactions among the dopant molecules or the failure of the lattice gas model.

Summary

While progress is being made towards the elucidation of the charge transport mechanism in molecularly doped polymer, much work remains. Our current focus is on understanding the origin of the initial spike and using a new experimental technique called TOF1A, in which the hole generation region is varied from the MDP surface to the entire bulk using e-beam excitation.

Acknowledgment

The authors would like to acknowledge many discussions with David Dunlap and Paul Parris.

References

[1] L. B. Schein, Andrey Tyutnev, "The Contribution of Energetic Disorder to Charge Transport in Molecularly Doped Polymers," J. Phys. Chem. C **112**, 7295 (2008).

[2] L. B. Schein, Vladimir Saenko, Evgenii D. Pozhidaev, Andrey Tyutnev, and D. S. Weiss, "Transient Conductivity Measurements in a Molecularly Doped Polymer Over Wide Dynamic Ranges," J. Phys. Chem. C **113**, 1067 (2009)

[3] L.B. Schein, D.S. Weiss, Andrey Tyutnev, "The Charge Carrier Mobility's Hopping Activation Energy and Pre-Factor Dependence on Dopant Concentration in Molecularly Doped Polymers," submitted

[4] L.B. Schein, "The Source of the Charge Transport Activation Energy in Molecularly Doped Polymers," Proceedings of NIP 24, p. 173 (2008).

[5] Private Communications: Jean-Luc Bredas, Veaceslav Coropceanu, and Seyhan Salman.

Authors Biography

Lawrence B. Schein received his Ph.D. in experimental solid state physics from the University of Illinois in 1970. He worked at the Xerox Corporation from 1970 to 1983 and at the IBM Corporation from 1983 to 1994. He is now an independent consultant. He has helped implement development systems in IBM laser printers, has proposed theories of most of the known electrophotographic development systems, and has

contributed to our understanding of toner charging, toner adhesion, and charge transport mechanisms in photoreceptors. He is the author of "Electrophotography and Development Physics," a Fellow of the American Physical Society, a Fellow of the Society of Imaging Science and Technology, recipient of the Carlson Memorial Award in 1993 and the Johann Gutenberg Prize in 2009, a Senior Member of the IEEE, and a member of the Electrostatics Society of America.

Andrey P. Tyutvev received his Master's degree in Radiation Chemisty from the Institute of Electrochemistry in 1977 and Ph.D. in Electrophysics and Physical Chemistry from the Institute of Chemical Physics in 1987 (both institutes of the Russian Academy of Sciences, Moscow). He worked at the Moscow Institute of Electromechanics from 1969 until now and at the Moscow Institute of Electronics and Mathematics (part time) from 1997. He spent his career working on radiation effects in polymer and ceramic insulators, studying the radiation-induced conductivity and bulk charging in them. During the last 10 years, he studied charge carrier transport in molecularly doped polymers using a novel radiation-induced variety of the time-of-flight method. He is the coauthor of 4 books on the subject (all in Russian).

David S. Weiss, a Senior Scientist at the University of Rochester, Rochester, NY, recently retired as a Scientist Fellow at the Eastman Kodak Company. He received his Ph.D. in chemistry from Columbia University (1969). His research focuses on organic electronic materials and devices with emphasis on organic photoreceptors for electrophotographic technologies. He holds 19 U.S. patents and is author of more than 90 publications. He is co-author of Organic Photoreceptors for Imaging Systems (Marcel Dekker, Inc., 1993), Organic Photoreceptors for Xerography (Marcel Dekker, Inc., 1998) and he is co-editor of the Handbook of Imaging Materials, Second Edition (Marcel Dekker, Inc., 2002). He was an Associate Editor of the Journal of Imaging Science and Technology from 1988-2008 and has served as General Chair of NIP17 and in many other NIP committee assignments. He is the Sponsorship Chair of NIP25/DF2009. In 1999 he received the Chester F. Carlson Award, in 2004 he was named an IS&T Senior Member, and in 2008 he was awarded IS&T Fellowship. In 2006 he was elected to the IS&T board as a vice-president and in 2008 he was elected as IS&T Treasurer

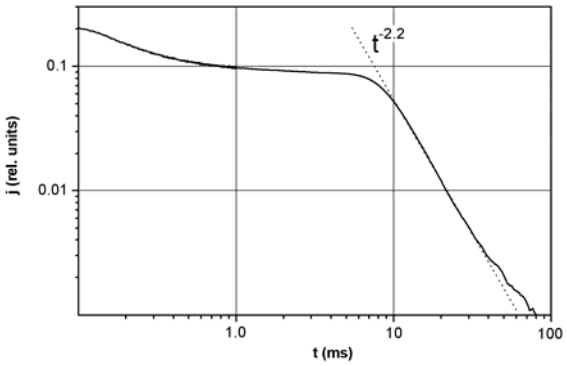

***Figure 2**. The current transient of Fig. 1 re-plotted on log-log axes.*

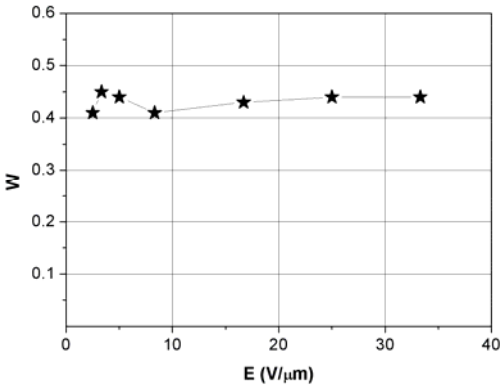

***Figure 3**. w (see text) vs. the electric field.*

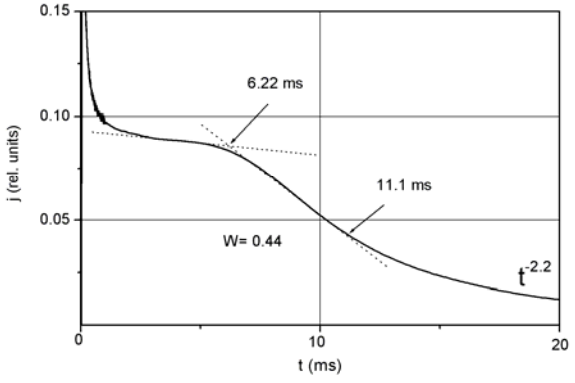

***Figure 1**. Current transient from holes which transit an MDP, 30%DEH (p-diethylaminobenzaldehyde diphenylhydrazone) in PC (bisphenol A polycarbonate) presented in linear current-linear time representation. The sample thickness was 18 microns and the electric field was 33 V/μm.*

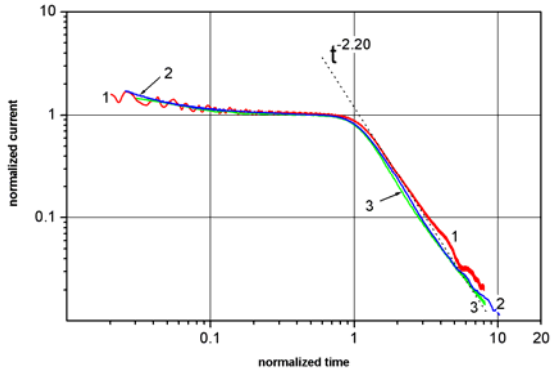

***Figure 4**. Log-log plots normalized to the transit time for three electric fields. 1 is 2.5 /μm, 2 is 8 V/μm and 3 is 33 V/μm. Note that the curves overlay within experimental error, demonstrating universality over very short times (including the spike) and very long times (consistent with w being field independent).*

Table 1. A complete list of activation energies of all MDP's which have been characterized as a function of dopant concentration in which the activation energy is <u>independent</u> of the dopant concentration.

		Dipole moment of dopant (D)	σ_{exp} (eV)	Δ_{exp} (eV)
Hole Transport				
1.	DTNA:PS	5.78	0.15	0.79
2.	DEASP:PS	4.34	0.11±3%	**0.61**
3.	DEASP:PC (E=30V/um)	4.34	0.11	**0.61**
4.	DEH:PS	3.16	0.13±4%	**0.60**
5.	DEH:PC	3.16	0.13	**0.60**
6.	DEH-A:PC	2.67	0.13	**0.60**
7.	DEH-B:PC	2.57	0.13	**0.60**
8.	DEH-C:PC	2.48	0.13	**0.60**
9.	TPM-E:PS	2.1	0.110	0.47
10.	TPA-4:PS	2.1	0.115	0.49
11.	TPA-3:PS	2.1	0.11	0.45
12.	TPA-2:PS	2.0	0.110	0.45
13.	TPM-D:PS	1.81	0.110	0.47
14.	TPM-C:PS	1.7	0.110	0.47
15.	TPM-B:PS	1.51	0.108	0.45
16.	PDA:MBDQ		≈1.4	**0.32**
17.	TPM:PS	1.33	0.122±.013	0.43
18.	TPM:PC	1.33	0.126±0.1	0.66
19.	TPA:PC	0.8	≈0.095	**0.30**
20.	TASB:PS	0.54	0.103	0.46
21.	DOA:PMPS	≈0.5	0.086	0.29
Electron Transport				
22.	DPQ:PS	0.4	0.118	0.52
23.	MBDQ:PCZ		0.5	**0.49**
24.	PTS:PC	2.2	0.134	0.57
25.	DCAQ:PC	3.3	0.132	0.63
26.	DCAQ:PS	3.3	0.132	0.63

Table 2 A complete list of activation energies of all MDP's which have been characterized as a function of dopant concentration in which the activation energy is <u>dependent</u> on the dopant concentration.

		Dipole moment of dopant (D)	σ_{exp} (eV)	Δ_{exp} (eV)
Hole Transport				
1.	TAA-A:PS	2.1	0.105-.115	0.43-0.52
2.	DPH:PCZ	≈2		**0.45-0.52**
3.	TPD:PC	1.52		**0.33-0.55**
4.	TPD:PS	1.52		**0.22-0.40**
5.	ETPD:PC	1.5		**1.32-0.45**
6.	ETPD:PS	1.5		**0.18-0.33**
7.	PDA:PC-Z	≈1.4		**0.35-0.60**
8.	TAPC:PC	1.0	0.090-0.136	0.31-0.70
9.	TAPC:PS	1.0	0.067-0.080 (E=30V/um)	---------
10.	ENA-B:PS	0.86	0.077-0.097	0.23-0.37
11.	ENA-C:PS	0.86	0.080-0.096	0.25-0.36
12.	TTA:PC	0.8	0.11-0.14	**0.40-0.60**
13.	TTA:PS	0.8	0.075-0.116	0.17-0.42
14.	TTA:PS-2	0.8	0.079-0.108	0.21-0.38
15.	TTA:PS-3	0.8	0.106-0.137	0.37-0.62
16.	ENA-A:PS	0.66	0.079-0.104	0.24-0.42
17.	ENA-D:PS	0.38	0.078-0.100	0.24-0.39

Definition of Initials used in this paper ("=" sign indicates different abbreviations of the chemical name are used for the same material)

DCAQ – 2-*t*-butyl-9,10-N,N'-dicyanoanthraguinonediimine
DEASP – 1-phenyl-3((diethylamino)styryl)-5-(*p*-(diethylamino)phenyl)pyrazoline
DEH – p-diethylaminobenzaldehyde diphenylhydrazone
DEH-A – 9-ethylcarbazole-3-carbaldehyde diphenylhydrazone
DEH-B – 9-ethylcarbazole-3-carbaldehyde methylphenylhydrazone
DEH-C – 1-pyrenecarbaldehyde diphenylhydrazone
DTNA – di-*p*-tolyl-*p*-nitrophenylamine
DOA – plasticizer dioctyl adipate
DPH – *p*-diphenyl-aminobenzaldehyde diphenylhydrazone
DPQ – 3,3'-dimethyl-5-5'-di-*t*-butyldiphenoquinone
ENA-A – N,N-bis(2-methyl-2-phenylvinyl)-N,N'-diphenylbenzidine
ENA-B – N-(2,2-diphenylvinyl)-4,4'-dimethyldiphenylamine
ENA-C – N,N-bis(2,2-diphenylvinyl)-N,N'diphenylbenzidine
ENA-D – N-(2,2-diphenylvinyl)diphenylamine
ETPD – N,N'-bis(4-methylphenyl)-N,N'-bis(4-ethylphenyl)-(3,3'-dimethylbiphenyl)-4,4'-diamine
MBDQ – 3,5-dimethyl-3',5'-di-*t*-butyl-4,4'-diphenoquinone
PC – bisphenol A polycarbonate
PCZ – poly(4,4'-cyclohexylidenediphenyl)carbonate
PDA – N,N,N',N'-tetrakis(m-methylphenyl)-1,3-diamino-benzene
PS – polystyrene
PS-2 – poly(4-*t*-butylstyrene)
PS-3 – poly(4-chlorostyrene)
PTS – 1,-dioxo-2-(4-methylphenyl)-6-phenyl-4-(dicyanomethylidene)thiopyran
TAA-A – ethyl ester of 4-[bis(4-methylphenyl)amino]benzenepropanoic acid
TAPC – 1,1-bis(di-4-tolylaminophenyl)cyclohexame
TASB – bis(ditolylaminostyryl)benzene
TPA – Triphenylamine
TPM = TPM-A=MPMP – bis(4-N,N-diethylamino-2-methylphenyl)-4-methylphenylmethane
TPM-B – bis(4-N,N-diethylamino-2-methylphenyl)(4-propylphenyl) methane
TPM-C – bis(4-N,N-diethylamino-2-methylphenyl)(4-phenylphenyl) methane
TPM-D – bis(4-N,N-diethylamino-2-methylphenyl)(4-phenyl) methane
TPM-E – bis(4-N,N-diethylamino-2-methylphenyl)(4-methoxyphenyl) methane
TTA = TPA-1 =TAA-1 - tri-*p*-tolylamine
TPA-2 = TAA-2 – tri-*p*-anisylamine
TPA-3 = TAA-3 – methyl 3-(*p*-(di-*p*-tolylamino)phenylpropionate
TPA-4 = TAA-4 – 4-bromo-4'4''-dimethyltriphenylamine
TPD – N,N'-diphenyl-N,N-bis(3-methylphenyl)-[1,1'-biphenyl]-4,4'diamine